ALTERNATIVE VALORISATION OF RED MUD AS CATALYST FOR SULPHIDE OXIDATION IN WASTEWATER

Rodica ZAVOIANU[1], Anca CRUCEANU[1], Octavian D. PAVEL[1], Luminiţa MARA[2], Teodor VELEA[2], Ruxandra BÎRJEGA[3]

[1] Department of Organic Chemistry, Biochemistry and Catalysis, Faculty of Chemistry, University of Bucharest, Bd. Regina Elisabeta No. 4-12, S3, 030018 Bucharest, Romania
[2] Institute of Research Development for Non-ferrous and Rare Metals - IMNR, Bd. Biruinţei No. 102, Pantelimon, Ilfov County, Romania
[3] National Institute for Plasma, Lasers and Radiation Physics-INFLPR Str. Atomiştilor, No. 409, cod 76900, PO Box MG 6, Măgurele, Ilfov County, Romania

rodica.zavoianu@g.unibuc.ro, anca.cruceanu@chimie.unibuc.ro, octavian.pavel@chimie.unibuc.ro, mara.luminita@gmail.com, tvelea@imnr.ro, ruxandra.birjega@inflpr.ro

Abstract

An alternative route for the valorisation of the bauxite residue (or so called "red mud") industrial waste as raw material in the manufacture of oxidation catalysts for wastewater treatment has been investigated. The catalysts were obtained by functionalisation of Fe(III) sites from bauxite residue (BR) with disodium ethylenediamminotetraacetic acid (H_2Na_2EDTA) and trisodium citrate (Na_3CIT). The catalysts were characterised by DRIFT, DR-UV-Vis, XRD, and BET porous structure determinations and their activity as well as their reusability in multiple cycles for sulphide oxidation was tested. The BR derived catalysts present good catalytic activity and reusability in oxidation reactions under mild reaction conditions and avoid the formation of FeS in treated wastewater.

Introduction

Alumina plants based on Bayer process yield besides the target product high amounts of an industrial waste called "red mud" or bauxite residue (about 1000-1500 kg for 1000 kg of alumina product). Usually the bauxite residue is deposited in landfill and its presence is harmful for the environment.[1] Lately, due to the more demanding environmental restrictions it has become necessary to find new ways to valorise this type of waste material. Some of the environmental-benign applications of bauxite residue applied until now are its use as: adsorbent for gas cleaning and wastewater treatment, building material additive, or source for metal recovery.[1,2]

The use of bauxite residue in water treatment has been limited so far to the removal of phosphate, arsenate or arsenite ions mostly using adsorption processes.[3,4]

Besides that, the alternative utilisation of bauxite residue (BR) as source for obtaining catalysts for hydrogenation, hydrodechlorination and hydrocarbon oxidation has also been explored.[5-9] Up to our knowledge, there are no published data concerning the catalytic activity of BR derived materials in the oxidation of sulphide ions from wastewaters. Sulphide ions are pollutants that occur in industrial wastewaters from oil refineries, fossil fuel gasification plants, paper and pulp mills, or after the anaerobic oxidation of sewage water. They may also be encountered in certain well waters. The sulphide ions from water have to be removed due to their toxicity and obnoxious odour. Recently, it has been attempted to use a BR aqueous suspension for the removal of H_2S from a gas stream by its conversion to FeS_2, FeS, $CaSO_4 \cdot 2H_2O$, sulphur, sulphide, and bisulphide of Na.[10] During this process, the pollutant is transferred from the gas phase both into the "red mud" solid which plays mainly the role of reagent and in the aqueous phase as soluble sulphur containing species.

As indicated by literature data,[1-10] both the raw and the activated bauxite residue contain also TiO_2, SiO_2, Al_2O_3 besides high amounts of Fe_2O_3. There are also references concerning the utilisation of iron oxide supported on TiO_2, SiO_2, Al_2O_3 or MgO as catalyst for the oxidation of sulphide ions to elementary sulphur in aqueous solutions.[11,12] Based on these informations, we have assumed that BR derived solids could be also active catalysts for the removal of sulphide ions from wastewaters. Therefore, this contribution concerns the valorisation of bauxite residue by its conversion into catalysts for oxidation processes using molecular oxygen as oxidising agent. The preparation method proposed for the obtaining of the BR derived catalysts involves the complexation (or so-called "functionalisation") of Fe(III) sites from bauxite residue by treatment with polycarboxylic acids. Even if the bauxite residue contains a multitude of metal sites it has been assumed that due to the higher stability constants of Fe complexes these would be preferentially formed[13]. This kind of treatment may preserve both the ability of Fe(III) to change the oxidation state during its involvement in the redox cycles as well as a sufficiently strong coordination in the ligands field in order to avoid the precipitation either as FeS_2 or $Fe(OH)_3$.[14]

Experimental

Preparation of catalysts

Bauxite residue (BR) deposit from Tulcea alumina plant in Romania has been utilised as raw material for the obtaining of iron containing catalysts. The chemical

composition of the BR as determined by ICP-AES and chemical analyses was: Fe (27 wt%), Al (10.5 wt%), Ti (4.4 wt%), Si (3.2 wt%), Na (3.7 wt%), K (0.25 wt%), Mg (0.3 wt%), Ca (4.4 wt%), Ba (0.2 wt%), O (42.8 wt%), C (1.3 wt%), H (0.4 wt%), F (0.25 wt%). This composition expressed as sum of oxides is: Fe_2O_3 (39.2 wt%), Al_2O_3 (20.2 wt%), TiO_2 (7.5 wt%), SiO_2 (7.0 wt%), Na_2O (5.1 wt%), K_2O (0.3 wt%), MgO (0.5 wt%), CaO (6.3 wt%), BaO (0.2 wt%), CO_3^{2-} (6.6 wt%), H_2O (6.9 wt%), (F concentration up to the balance of 100 wt%). The following catalysts have been prepared by functionalisation of trivalent iron sites from bauxite residue following a treatment with polycarboxylic acids: BR-E (BR modified with H_2Na_2EDTA solution), BR-C (BR modified with Na_3CIT solution) and BR-E-C (BR modified with both H_2Na_2EDTA and Na_3CIT solutions). The concentration of polycarboxylic acid salt solution was calculated based on the amount of Fe in the BR enabling a molar ratio H_2Na_2EDTA/Fe and Na_3CIT/Fe of 1-1.5 and respectively, 1-2. The bauxite residue was submitted to contact with the corresponding sodium salts solutions (weight ratio L/S=10:1) at room temperature during 144 h under intermittent gentle stirring (150 rpm). Afterwards, the solid separated by filtration, was washed with distilled water until the conductivity of the water decreased below 100 µS/cm and dried at 60 ^{o}C during 24 h. The waste waters were analysed in order to determine the concentration of metal cations solubilised from the bauxite residue during the treatment with polycarboxylic acids. Na content in the waste water analysis was disregarded since it could come both from the BR or the functionalisation agent.

Catalysts characterisation

The catalysts were characterised by DRIFT, DR-UV-Vis, XRD, and BET porous structure determinations. DRIFT spectra in the range 4000-400 cm^{-1} were collected with a Varian 3100 Excalibur spectrometer equipped with diffuse reflectance accessory Harrick Praying Mantis. The spectra were averaged over 200 scans and refined by subtracting the KBr spectrum used as background. DR-UV-Vis NIR spectra in the range of 200-2600 nm were recorded with a Shimadzu UV-3600 spectrophotometer equipped with an integrating sphere. Obtained DR-UV–VIS –NIR spectra were finally corrected using the Kubelka-Munk transformation ($f(R) = (1-R)^2/(2R) = K/S$, where R is the absolute reflectance, K and S are the absorption and scattering coefficients).[15] XRD patterns were obtained on Schimadzu XRD 7000 diffractometer using Cu Kα radiation (λ = 1.5418 Å, 40 kV, 40 mA) at a scanning speed of 0.10° min^{-1} in the 5–70° 2θ range. The characterisation of the porous texture of BR sample was performed by N_2 adsorption at -196 °C using a Micrometrics instrument (ASAP 2010). The Brunauer-Emmett-Teller (BET) method was used to calculate the surface area from the data obtained at P/P_0 between 0.01 and 0.995. Prior to surface area determination, the sample was outgassed at 150 °C for 5 h. The pore size distribution was determined from the desorption branch of the N_2 isotherm, using Barrett-Joyner-Halenda (BJH) formalism.[16]

Catalytic activity tests

The tests for the oxidation of sulphide by oxygen from air were performed at ambient temperature and pressure, under continuous stirring (350 rpm), using an experimental set-up consisting of a two-necked glass flask reactor equipped with a teflon-coated stirrer bar, a gas-inlet tubing connected to a dry air supplier and a reflux condenser. The standard operating conditions were: 4l/h air flow, 1.3 wt% of catalyst in sulphide containing wastewater (S^{2-} initial concentration $C_{0,S^{2-}}$ = 1 g/l), 2 hours reaction time. The synthetic wastewater (1 g S^{2-}/l) was freshly prepared by dissolving an adequate amount of $Na_2S \cdot 9\ H_2O$ in deoxygenated distilled water. The stability of the catalysts under operating conditions and their reusability was investigated by performing 10 reaction cycles (2 h each) using the same catalyst which was separated by filtration from the reaction mixture at the end of each cycle, and was contacted with a fresh sample of sulphide containing wastewater in the next cycle under the same operating conditions.

Results and Discussion

Structural characterisation of the catalysts

The XRD patterns of the investigated samples (Figure 1) showed that all the samples contained a mixture of crystallographic phases. The semiquantitative phase analysis for BR sample gave the following composition in wt%: 30.2 hematite (PDF 1-087-1164), 9.7 goethite (PDF 01-081-0464), 7.5 diaspore (PDF 01-084-0175), 2.3 bohemite (PDF 01-083-1505), 10.5 gibbsite (PDF 01-074-1775), 9.2 calcite (PDF r01-071-3699), 2.2 rutile (PDF 01-070-7347), 0.7 anatase (PDF 00-021-1272), 7.7 cancrinite (PDF 01-089-8592), 11.4 cancrisilite (PDF 01-089-8047), 4.7 hydrogarnet (PDF 00-032-0147), 1.9 muscovite (PDF 00-007-0042), 2.1 amesite (PDF 01-087-2057).[17] The XRD patterns of the functionalised BR samples showed that the characteristic diffraction lines of hematite are preserved indicating that there is a low solubilisation of iron species. An interesting aspect is that all the diffraction lines are more intense than in the pattern of BR suggesting that some amorphous phases from the bauxite residue were removed by solubilisation. Also, there are several new bands corresponding to the complexes formed on the surface of BR. For BR-E the new diffraction lines appeared at: 9.88°, 21.43° and 42.5°, for BR-C at 21.51°, 26.64° and 39.33° while for BR-E-C the new lines were 21.27°, 21.51°, 26.49°, 34.37° 38.84° and 42.34°. The treatment with polycarboxylic acids lead to a preferential solubilisation of Al, Ca and Mg from the bauxite residue since in the diffraction patterns of the functionalised samples the characteristic diffraction lines for amesite (A) and bohemite(B) are missing, while the line corresponding to muscovite (M) has lower intensities. Also, the third diffraction line characteristic to gibbsite (GB) is

missing in the XRD patterns of BR-C and BR-E-C. Besides that, there is an important decrease of intensity for the calcite (CA) phase or BR-E-C sample.

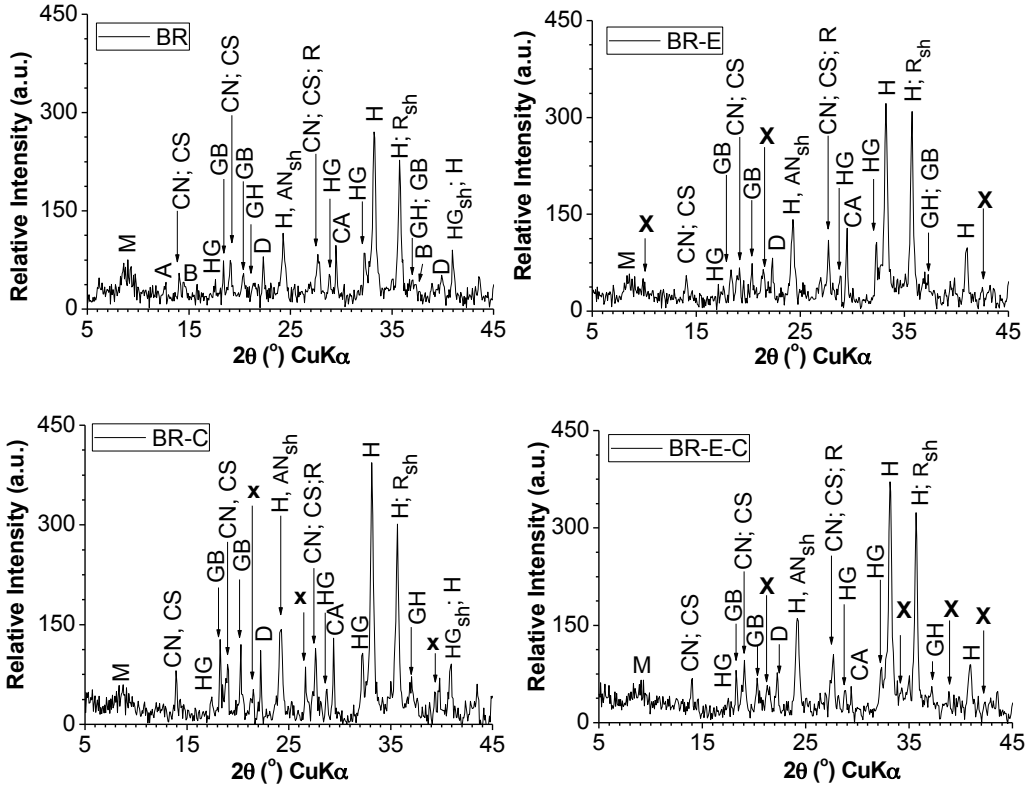

Figure 1: Powder X-ray diffractograms of untreated bauxite residue (BR) and the samples functionalised with carboxylic acids: BR-E; BR-C and BR-E-C (H-hematite (Fe_2O_3), HG-hydrogarnet ($Ca_3Al_2(O_4H_4)_3$); CA-calcite ($CaCO_3$); D-diaspore (α-Al(O)OH); GB-gibbsite ($Al(OH)_3$); GH-goethite (FeO(OH)); CN-cancrinite ($Na_6Ca_2[(CO_3)_2|Al_6Si_6O_{24}]\cdot 2H_2O$), CS-cancrisilite ($Na_7(Al_5Si_7O_{24})(CO_3)\cdot 3H_2O$); A-amesite ($Mg_2Al_2SiO_5(OH)_4$); B-bohemite (γ-Al(O)OH); M-muscovite ($KAl_2(AlSi_3O_{10})(F,OH)_2$); AN-anatase ($TiO_2$); R-rutile ($TiO_2$); X - complex); sh- shoulder

The hypothesis of the partial solubilisation was confirmed by the results of the chemical analyses of the waste waters obtained after the treatment with polycarboxylic acids, which are displayed in Table 1.

Table 1: Metal content in the waste waters obtained after the synthesis of BR-E, BR-C and BR-E-C catalysts (10 grams of BR were utilised for each synthesis)

	Volume of waste water	Concentration (mg/l)[#]					
Sample	(litre)	Fe	Al	K	Mg	Ca	Ba
BR-E	0.920	1.2	533.4	0.5	32.2	230.7	1.6
BR-C	0.945	1.4	532.4	0.4	31.1	122.2	1.3
BR-E-C	0.960	1.0	529.9	0.3	33.3	354.6	1.7

[#] Ti and Si were under detection limit

The normalised DR-UV-Vis NIR spectra of the BR derived samples are presented in Figure 2.

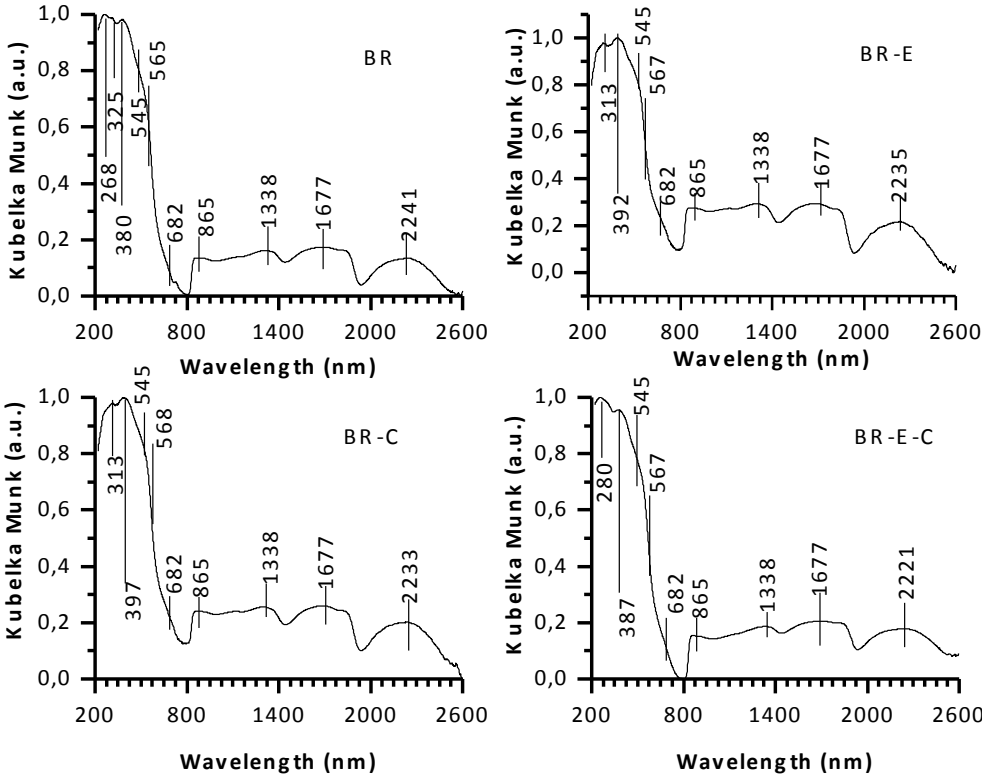

Figure 2: Normalised DR-UV-Vis NIR spectra of untreated bauxite residue (BR) and the samples functionalised with carboxylic acids: BR-E; BR-C and BR-E-C

Due to the complex composition of the solids the bands are diffuse and they overlap. Therefore it was necessary to apply the deconvolution[18] as well as the first derivative method[19] in order to perform the component analysis. Using this method we could identify several absorption bands corresponding to Fe^{3+} in octahedral symmetry at: 865 nm ($^6A_{1g}(S) \rightarrow {}^4T_{1g}(G)$ transitions), 682 nm ($^6A_{1g}(S) \rightarrow {}^4T_{2g}(G)$ transitions), 565-568

and 545 nm ($^6A_{1g}(S) \rightarrow {}^4E_g$, $^4A_{1g}$ (G) transitions in Hematite and Goethite), 445 nm ($^6A_{1g}(S) \rightarrow {}^4T_{2g}(D)$ in Hematite), 325 nm (pair excitation $^6A_1 + {}^6A_1 \rightarrow {}^4T_2(^4G) + {}^4T_2(^4G)$), 313 nm ($^6A_{1g}(S) \rightarrow {}^4T_{1g}(P)$), 280 nm (ligand to metal charge transitions).[15, 17-19] For BR-E and BR-C samples the most intense absorption is noticed in the region corresponding to the ligand field transitions of metal cations (around 400 nm) whereas for BR and BR-E-C the most intense absorption is noticed in the region corresponding to ligand to metal charge transitions which are centered below 300 nm. Therefore it may be concluded that following the complexation of the red mud with one type of polycarboxylic acid, there is a stronger stabilisation of metal cations in the ligand field. At first glance, the complexation with polycarboxylic acids leads to an increased intensity of the absorption bands in the NIR region of the spectra compared to the neat BR. For BR and BR-E-C the maximum absorption (0.17 and 0.20 relative intensity) is noticed in the region corresponding to the bands of the hydroxyl-stretching and deformation vibrations (1400-1800 nm). Meanwhile for BR-E and BR-C the band corresponding to the overtones of OH stretching centered at 1338 nm has the same maximum relative intensity as the band situated in the region 1400-1800 nm. In the spectrum of BR, the maximum relative intensity of the absorption in the region 2000-2600 nm related to the presence of combination and overtone modes of carbonate[16,18] is 0.13. Due to the presence of the polycarboxylic ligands, in the spectra of BR-E, BR-C and BR-E-C the maximum relative intensity of the absorption in this region is 0.18 for BR-E, 0.69 for BR-E-C and 0.15 for BR-C. The variation of the relative intensity of this maximum may be related to the concentration of carboxylate species in the ligands utilised to functionalise the BR samples considering the number of carboxylic groups in NaH_2EDTA (4), in Na_3Cit (3) and their relative contribution in the preparation of BR-E-C solid.

The effect of the functionalisation with polycarboxylic acids was clearly proved by the different spectral characteristics of the samples in the region 1800-400 cm^{-1} of the DRIFT spectra (Figure 3).

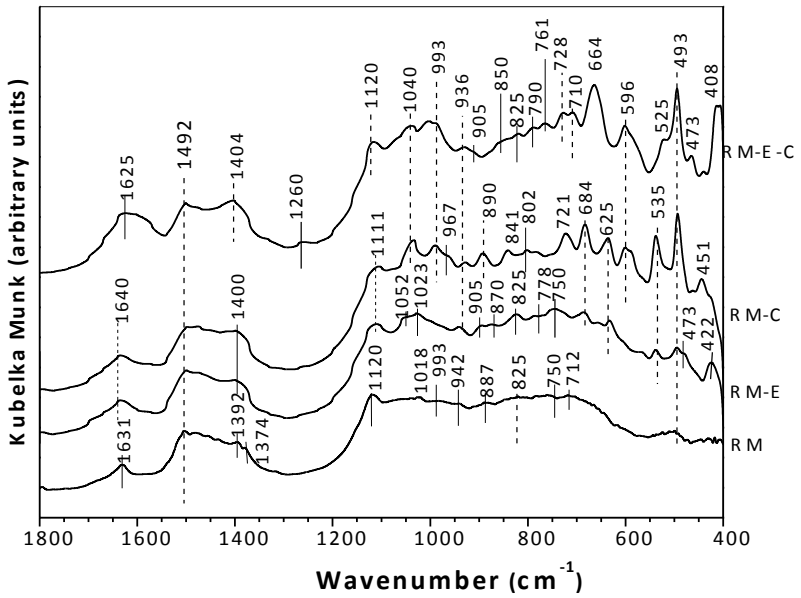

Figure 3: DRIFT spectra of the samples in the region 1800 - 400 cm^{-1}

In the region 1800-1000 cm^{-1}, the symmetric carboxyl stretching band appears near 1400 cm^{-1} in the spectra of EDTA salts. This band was present in all the spectra of functionalised samples. The shifting of this band to 1404 cm^{-1} in the spectrum of BR-E-C indicates an enhanced symmetry of the carboxylate group in this sample.[21] Meanwhile, in the spectrum of BR there is a band characteristic to carbonate anions at 1392 cm^{-1}. The complexation of the metal cations with the carboxylic acids was also indicated by the absence of the bands at 1720 cm^{-1} (typical for C = O in COOH) and 1200 cm^{-1} (C-O stretch of OH-deformation of COOH) which also indicates the presence of ionised carboxylate COO^- groups.[22] Only BR-E-C spectrum shows the band at 1260 cm^{-1} characteristic for the symmetric stretching of COO^- group when carboxyl acts as a monodentate ligand.[23] The presence of this band is accompanied by an increase of intensity and width of the band corresponding to the asymmetric stretching of COO^- group at 1640 cm^{-1}. Besides that, in the spectrum of BR-E-C, there are other spectral modifications indicating either the perturbation of Fe(III)EDTA by the concomitant presence of the citrate anion, or the complexation of the citrate anion with Fe(III)-EDTA chelate which would mean that the iron would be coordinated by two oxygen atoms belonging to different sources. These modifications are: the shifting of the weak band around 800 cm^{-1}, related to Fe-O-Fe bonds vibrations in the iron citrate to 850 cm^{-1}, and an intense band at 663 cm^{-1}, which is shifted compared to the band at 625 cm^{-1} characteristic to iron citrate.[14,24] The bands characteristic for deformation vibrations of OH appear at 1120, 1018, 887, 759 cm^{-1} in the BR spectrum. The position of the band at 1018 cm^{-1} is shifted toward higher wavenumbers in the spectra of BR-E (1023 cm^{-1}), BR-C and BR-E-C (1040 cm^{-1}) indicating an increased strength of the bond in the functionalised bauxite residue.

All spectra presented also the bands typical for Al-O out-of-plane and Al-O-Si in-plane vibrations[25] located at 825 and 759 cm^{-1}. In the spectrum of BR-C the position of these two bands is shifted at 841 and 721 cm^{-1}, while in the spectrum of BR-E-C only the band at 759 cm^{-1} is shifted to 761 cm^{-1}. Only the spectra of BR-E and BR-E-C show the band at 473 cm^{-1} characteristic for ν(Fe-N) vibrations[23] which proves the formation of Fe(III)EDTA chelate. The presence of superficial silicate groups indicated by characteristic bands for Si—O (993 cm^{-1})[10] is noticed only for BR, BR-C and BR-E-C. Taking into account that this band is missing in the spectrum of BR-E it may be suposed that the chelates formed during the treatment with H_2Na_2EDTA covered better the external surface of the bauxite residue particles.

Catalytic activity testing

The results of the catalytic tests for sulphide oxidation by air are presented in Table 2. It may be seen that the bauxite residue itself has a poor catalytic activity in this process since the conversion did not exceed 10 % even in the first reaction cycle. The functionalisation of the bauxite residue with polycarboxylic compounds enhances its catalytic activity. Compared to BR, the sample BR-C functionalised with Na_3Cit is twice more active, the sample BR-E treated with H_2Na_2EDTA is 5 times more active, while the sample BR-E-C treated with the mixture of Na_3Cit and H_2Na_2EDTA is almost 10 times more active in the first reaction cycle. This increase of catalytic activity may be a consequence of the presence of iron chelates formed on the surface of the bauxite residue following its treatment with polycarboxylic compounds as it was also revealed by the structural analyses of the catalysts. Another consequence of the functionalisation is that during this process a part of the amorphous phases from the bauxite residue were removed by solubilisation. Both the dissolution process and the formation of the complexes on the surface of the bauxite residue particles influenced the textural properties of the resulting solid as it may be seen from the results presented in Table 3.

Table 2: The results obtained in the catalytic tests for the oxidation of sulphide ions from wastewater (Reaction conditions: 25 ^{o}C, stirring 350 rpm, 4 l/h air flow, 1.3 wt% of catalyst in wastewater (S^{2-} initial concentration $C_{0,S^{2-}}$ = 1 g/l), 2 h reaction time)

	Sulphide conversion (%)									
Cycle / Catalyst	1	2	3	4	5	6	7	8	9	10
BR	7.8	7.5	7.1	6.6	6.0	5.8	5.2	4.7	4.1	3.7
BR-E	37.1	36.8	36.1	35.2	32.1	28.2	24.3	19.5	17.2	16.5
BR-C	16.7	16.2	15.7	15.1	14.5	12.7	10.6	9.1	8.3	7.1
BR-E-C	70.0	69.7	69.0	69.0	68.5	68.2	67.2	66.3	64.5	62.2

Table 3: Textural characteristics of the samples

Sample	BET Specific surface area S_{sp} (m^2g^{-1})	BJH Adsorption cumulative volume of pores (cm^3g^{-1})	BJH Average pore diameter (4V/A) (Å)
BR	13	0.082	237.4
BR-E	43	0.215	220.2
BR-C	22	0.141	228.7
BR-E-C	65	0.415	212.3

The surface area of the BR ($13\ m^2\ g^{-1}$) is sensible lower than that of the functionalised samples. This fact is due do the presence of macropores with diameters over 500 Å in this type of solid. The increase of the surface area after functionalisation is mainly due to the adsorption of the newly formed chelates on BR surface, which generates an increase of the micropores amount. Consequently there is also a decrease of the average pore diameter. The results of the textural analysis are well correlated to the catalytic activity of the solids showing that the catalytic activity increases along with the specific surface area of the catalyst.

The results obtained after the testing of the catalysts in multiple reaction cycles (Table 2) showed that only the sample BR-E-C was able to maintain its high activity over a long number of cycles. The stability of the catalysts decreases following the same order as their catalytic activity: BR-E-C > BR-E > BR-C > BR.

Conclusions

The obtained results showed that the functionalisation of the bauxite residue with disodium ethylenediamminotetraacetic acid (H_2Na_2EDTA) or/and trisodium citrate (Na_3CIT) yields active catalysts for the oxidation of sulphide ions from wastewaters using air as oxidation agent.

The proposed preparation method presents the advantage that besides the formation of Fe(III) complexes on the surface of the bauxite residue, it allows also the re-adsorption of the complexes formed in the solution following the dissolution of Fe by the complexation agents. This process that occurs during the preparation step leads to an increase of the surface area of the functionalised catalysts.

The most promissing catalyst BR-E-C was obtained using a mixture of H_2Na_2EDTA and Na_3CIT as complexation agents. The advantage brought by the use of both chelating agents consists in the obtaining of a complex structure which is less stable in the ligand field compared to BR-E or BR-C and therefore has a better ability to change its

geometry and can participate easier to ligand exchanges which are of crucial importance for its catalytic activity.

Acknowledgements

Authors acknowledge the financial support of this work by UEFISCDI through PCCA2 project 78/2014.

References

1. S. Kumar, R. Kumar and A. Bandopadhyay, "Innovative Methodologies for the Utilisation of Wastes from Metallurgical and Allied Industries", *Resour. Conserv. Recy.*, **48** 301–314 (2006).
2. S. Wang, H. M. Ang and M. O. Tadé, "Novel Applications of Red Mud as Coagulant, Adsorbent and Catalyst for Environmentally Benign Processes ", *Chemosphere,* **72** 1621-1635 (2008).
3. H. Genc, J. C. Tjell, D. McConchie, and O. Schuiling, ''Adsorption of Arsenate from Water Using Neutralized Red Mud" *J. Colloid. Interface Sci.*, **264** 327–334 (2003).
4. J. Pradhan, J. Das., S. Das and R. S. Thakurl "Adsorption of Phosphate from Aqueous Solution Using Activated Red Mud" *J. Colloid. Interface Sci.*, **204** 169-172 (1998).
5. J. R. Paredes, S. Ordóñez, A. Vega and F. V. Díez, "Catalytic Combustion of Methane Over Red Mud-Based Catalysts*" Appl. Catal. B: Environmental,* **47** 37–45 (2004).
6. K. C. Pratt and V. Christoverson, "Hydrogenation of a Model Hydrogen-Donor System Using Activated Red Mud Catalyst", *Fuel*, **61** 460–462 (1982).
7. S. Ordóñez, F.V. Díez and H. Sastre, "Hydrodechlorination of Tetrachloroethylene Over Sulfided Catalysts: Kinetic Study*", Catal. Today,* **73** 325–331 (2002).
8. S. Ordóñez, H. Sastre and F.V. Díez, "Catalytic Hydrodechlorination of Tetrachloroethylene Over Red Mud", *J. Hazard. Mater.*, **81** 103–114 (2001).
9. J. F. Lamonier, F. Wyralski, G. Leclercq, and A. Aboukais, "Recycling of Waste, Red Mud, As a Catalyser for the Elimination of Volatile Organic Compounds"*, Can. J. Chem. Eng.,* **83** 737–741 (2005).
10. R. C. Sahu, R. Patel and B. C. Ray, "Removal of Hydrogen Sulfide Using Red Mud at Ambient Conditions", *Fuel Processing Technology,* **92** 1587-1592 (2011).
11. R. J. A. M. Terorde, P. J. van den Brink, L. M. Visser, A. J. van Dillen, and J.W. Geus, "Selective Oxidation of Hydrogen Sulfide to Elemental Sulfur Using Iron Oxide Catalysts on Various Supports", *Catal. Today*, **17** 217-225 (1993).
12. K. D. Jung, O. S. Joo, S. H. Cho, S. H. Han, "Catalytic Wet Oxidation of H_2S to Sulfur on Fe/MgO Catalyst"*, Appl. Catal. A: General,* **240** 235-241 (2003).
13. **http://maxchelator.stanford.edu/xlsconstants.htm**: 10/14/2002 for files of constants in: CMC1002S.TCM CMC1002E.TCM CMC1002S.CCM CMC1002E.CCM.
14. A. Cruceanu, R. Zavoianu, and E. Angelescu, E., "Catalytic Desulphurisation of Gaseous Streams Containing H_2S in the Presence of Fe, Co and Cr Chelates Catalysts", *Prog. Catal.*, **10** (1-2) 27-39 (2001).
15. R. G. J. Strens, and B. J. Wood, "Diffuse Reflectance Spectra And Optical Properties Of Some Iron And Titanium Oxides And Oxyhydroxides", *Mineralogical Magazine*, **43** 347-354 (1979).
16. E. P. Barrett, L. G. Joyner, and P. P. Halenda, "The Determination of Pore Volume and Area Distributions in Porous Substances. I. Computations form Nitrogen Isotherms". *J. Am. Chem. Soc.,* **73** (1) 373–380 (1951).
17. ICDD database, Powder Diffraction File, edited by International Centre for Diffraction Data 2006.

18. S. J. Palmer, C. Ray and R. L. Frost, ”Characterisation of Bauxite and Seawater Neutralised Bauxite Residue Using XRD and Vibrational Spectroscopic Techniques”, *J. Mater. Sci.,* **44** 55–63 (2009).
19. W. Zhou, L. Chen, M. Zhou, W. L. Balsma and J. Ji, ”Thermal Identification Of Goethite In Soils And Sediments By Diffuse Reflectance Spectroscopy”, *Geoderma*, **155** (3-4) 419-425 (2010).
20. D. M. Sherman, T. D. Waite, ”Electronic Spectra of Fe^{3+} Oxides and Oxide Hydroxides in the Near IR to Near UV”, *American Mineralogist*, **70** 1262-1269 (1985).
21. K. C. Lanigan and K. Pidsosny, “Reflectance FTIR Spectroscopic Analysis of Metal Complexation to EDTA and EDDS”, *Vibrational Spectroscopy,* **45** 2–9 (2007).
22. G. S. R. Krishnamurti and P. M. Huang, “Influence of Citrate on the Kinetics of Fe(II) Oxidation and the Formation of Iron Oxyhydroxides 1”, *Clay Clay Miner.,* **39** (1) 28-34 (1991).
23. J. Ryczkowski, “IR Studies of EDTA Alkaline Salts Interaction with the Surface of Inorganic Oxides”, *Appl. Surf. Sci.***, 252** 813–822 (2005).
24. C. C. Wagner and E. J. Baran, “Vibrational Spectra of Two Fe(III)EDTA Complexes Useful for Iron Supplementation”, *Spectrochim. Acta Mol. Biomol. Spectros.,* **75** 807-810 (2010).
25. J. D. Russell, ”Infrared Spectroscopy of Inorganic Compounds” in *Laboratory Methods in Infrared Spectroscopy,* Edited by H. Willis, Wiley, New York, 1987.